

# SPACE CHARGE RESONANCE ANALYSIS AT THE INTEGER TUNE FOR THE CERN PS

F. Asvesta and F. Schmidt, CERN, Geneva, Switzerland

## Abstract

In the context of the LHC Injectors Upgrade (LIU) project, a series of studies have been performed in order to better understand the beam brightness limitations imposed by resonances and space charge effects.

Space charge simulations using the adaptive space charge solver as implemented in the MAD-X code conducted for the CERN Proton Synchrotron (PS) show that a particle approaching the integer tune of  $Q_x = 6$  demonstrates a resonant behavior. The analysis of the single particle transverse motion reveals the excitation of a second order resonance. The interplay of the space charge effect and the optics perturbation in the regime of the integer tune on this excitation was further investigated. The simulations were complemented with the analysis of the resonance driving terms coming from the space charge potential derived in a classical perturbative approach.

## INTRODUCTION

The space charge is a dominant effect in high brightness low energy machines like the CERN PS. In this respect, multiple studies were conducted in order to understand the limitations for pushing the brightness in the scope of the LHC Injectors Upgrade (LIU) project [1]. Numerous studies, have shown that the available tune space in the PS is limited by both machine error and space charge driven resonances [2–6]. With such a limited transverse tune space, there is a need to better understand the impact of the integer resonance on the beam and investigate the sources of the excitation [7].

Experimental and simulation studies have been performed at the CERN PS to understand space charge effects in conjunction with sextupole non-linearities [3], including tune working points that sample a sextupole resonance but also the integer resonance. The minimum horizontal bare machine tune used in experiments and simulations alike was  $Q_x = 6.039$ , i.e. slightly above the integer while the maximum horizontal incoherent tune spread was  $-0.05$ . For the simulations discussed in this paper the code used is MADX-SC, an extension of the MAD-X Ref. [8] code including a space charge (SC) implementation of the adaptive mode. MADX-SC is presented in more details in Ref. [9] at this workshop.

For the SC studies presented here, the MADX-SC adaptive mode was selected, in which the beam emittances are re-calculated from the particle distribution at each turn in order to adapt the SC kicks accordingly. The analytical solvers allow simulating just a few 1'000 macro-particles and is therefore the only way to reach long periods, e.g. 500'000 turns for the typical CERN PS storage time. However, the

SC force recalculations of the adaptive mode introduces some noise to the beam that needs to be minimized by increasing the number of macro-particles. For the PS simulation we had to increase the number of macro-particles from 1'000 to 2'000 to reduce the noise to an acceptable level [9]. This has to be seen as a compromise between simulation speed and artificial emittance blow-up, although this is much less of a problem than for the Particle In Cell (PIC) simulations [10–12]. It should be noted that MADX-SC also has a self-consistent mode but its much larger noise levels and longer simulation times make it impractical for most applications.

The simulation results will be discussed taking into account the PS complexity concerning matching of the tunes. The PS is a machine with combined function magnets with additional circuits for Pole Face Windings (PFWs). The combined function magnets define the transverse tune space that is accessible for the PS while the PFWs and additional quadrupoles, namely the Low Energy Quadrupoles (LEQs), can be used for fine adjustment of the tunes. The perturbations of the optics, when different combinations of the above elements are used, have an impact on resonance excitation in the presence of the space charge force.

In the first section, the analysis of the resonance structure found in phase space during the simulations will be presented. In the second section, the nature of the excitation of this higher order resonance on the integer tune will be discussed using the calculation of the resonance driving terms coming from the space charge potential and the harmonic analysis of the beam size and hence the beta functions as the integer resonance is approached.

## RESONANCE ISLANDS IN SIMULATIONS

MADX-SC simulations are conducted for a working point close to the integer tune,  $Q_x = 6.039$  and  $Q_y = 6.479$  with the beam parameters shown in Table 1. To this end, a particle distribution of 2'000 macro particles is chosen to minimize numerical noise. A single particle that basically sits in the center of the bunch with very small initial coordinates is added to the 2'000 particle distribution. This special particle can be considered as a probe particle that is influenced by the full beam but itself affects very little the other particles of the bunch. Therefore, this particle is very close to the closed orbit and can be used to determine the maximum SC tune shift by analyzing its turn-by-turn motion.

### *Tune Matching as in the Experiment*

In this section we are using the PFW for a large shift of the working point from the base tunes. The fine-tuning towards the horizontal integer and the vertical half integer

tunes is done via the LEQ families. This is very close to the procedure used in the 2012 PS experiment [3].

Table 1: Beam Characteristics for the Simulations and the Calculation of the RDTs Shown in Fig. 6

Kinetic energy	2 GeV
Intensity [ $1 \times 10^{10}$ ppb]	55
Bunch length (rms) [m]	9.59
Momentum spread $\Delta p/p$ (rms) [ $10^{-3}$ ]	0.95
Hor. normalized emittance, $\varepsilon_x^n$ ( $1\sigma$ ) [ $\mu\text{m}$ ]	3.5
Ver. normalized emittance, $\varepsilon_y^n$ ( $1\sigma$ ) [ $\mu\text{m}$ ]	2.2
Horizontal tune shift, $\Delta Q_x$	-0.05
Vertical tune shift, $\Delta Q_y$	-0.07

In the following we examine the phase space topology by inspecting the phase space trajectories for individual particles. In particular, particles are launched with different initial horizontal offsets from the closed orbit, while in the vertical and the longitudinal planes the initial conditions were chosen very close to the closed orbit. Different particle trajectories will be shown in different colors. In all phase space plots (Figs. 1 to 5) the coordinates follow the MAD-X convention.

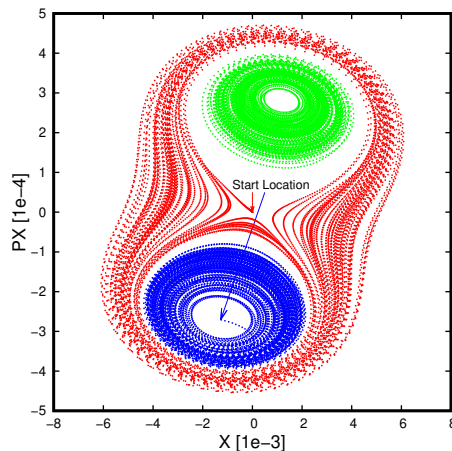


Figure 1: Horizontal Phase Space for three particles: Tiny initial amplitude with chaotic motion (red); Upper Island (green) and Lower Island (blue). Red and blue arrows point to the tiny initial amplitude and the initial coordinates of the lower island respectively.

In Fig. 1 one finds in red the horizontal phase space for a particle launched close to zero amplitude, where the red arrow points to the horizontal starting point. The particles shown in blue and in green are launched with an offset and exhibit the motion inside an “upper” (green) and a “lower” (blue) island. For the lower island the starting locations is indicated by a blue arrow.

In Fig. 2 one finds the corresponding traces in the longitudinal phase space.

At this point a few explanations are needed: in the horizontal plane the zero amplitude has become the unstable fixed point of the second order resonance and the motion

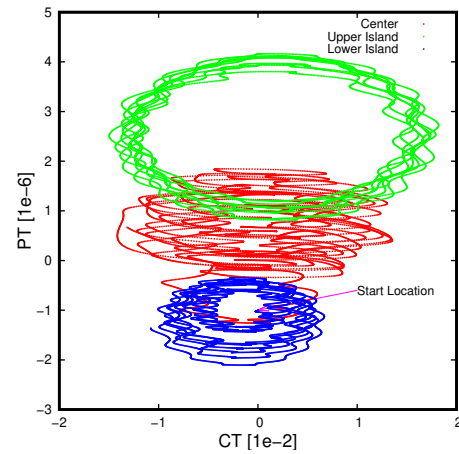


Figure 2: Longitudinal Phase Space for three particles: Tiny initial amplitude with chaotic motion (red); Upper Island (green) and Lower Island (blue). The arrow, magenta for visibility, is pointing to the start location of the Lower Island.

evolves around the separatrix, which by nature is chaotic. On the other hand, the island cases, while existing for at least 10'000 turns are not truly stable, but should be called meta-stable at best. This might happen just due to the fact that other effects like the sextupole non-linearities also drive this or other resonances at the integer; the strong coupling between horizontal and longitudinal phase space due to horizontal dispersion which is further enhanced by SC; or the fact that in the adaptive mode noise is being introduced. The latter is discussed below.

Figures 1 and 2 seem to suggest that one may just zoom into the respective horizontal and longitudinal islands to find the stable island fixed points. In practice, it turns out that it is exceedingly difficult to do just that. Instead it becomes an elaborate search in 4D (apparently it does not depend on the vertical plane). The limitation of this attempt becomes apparent in the 2 figures for the lower island: the starting location in both plots seem to be close to the center of either island, yet this area seems not stably accessible.

In Ref. [13] it had been shown that the four-fold increase of the number of macro-particles leads to the statistical reduction of the noise by a factor of 2. Therefore the upper island simulations have been repeated with a factor 5 increased number of macro-particles (i.e. 10k instead of 2k), since the simulations can still be done reasonably fast. In Fig. 3 one finds that the jittery islands MOP20.images are even more enhanced for the higher number of macro-particles. This does not prove that this kind of noise is unimportant for particle stability but it does seem more likely that the internal non-linear dynamics are causing this meta-stable particle behavior.

We do not show here the vertical phase space since it is not coupled to either of the other two planes.

It needs to be mentioned that in parallel, M. Titze has performed separate studies for his PhD at the PS under slightly different conditions [14]. He did find similar indications of

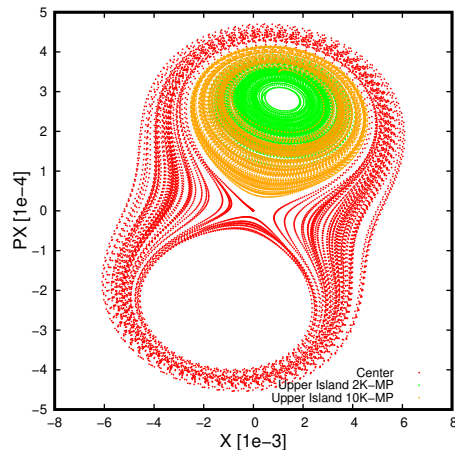


Figure 3: Noise test in Horizontal Phase Space for three particles: Tiny initial amplitude with chaotic motion (red) as in Fig. 1; Upper Island (green) as in Fig. 1. In orange one finds the result for the same initial coordinates of the upper Island but with 5 times larger number of macro-particles.

a resonant behavior but did not include a full analysis in his thesis.

### Tune Matching with the PFW System Only

Knowing about the limitations of the LEQ system [7] we have attempted a tune matching with just the PFW system.

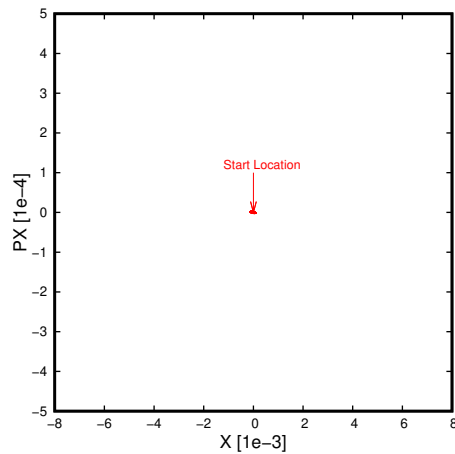


Figure 4: PFW System: Horizontal Phase Space with the red arrow to the tiny initial amplitude, keeping the same scale as in Fig. 1.

In Fig. 4, showing the horizontal plane, the arrow points again to the tiny initial amplitude, but this time the amplitude remains tiny and is hardly visible since we have kept the same scale as in Fig. 1. In Fig. 5 one finds the longitudinal phase space that occupies about the same area in the longitudinal phase as in Fig. 2, but here one can no longer find the jittery motion that is due to the strong coupling with the horizontal plane.

Thus it seems that the use of the LEQs leads to the resonance behavior, presumably due to the interplay of the

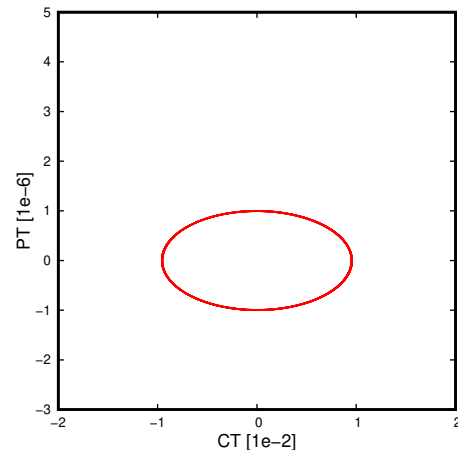


Figure 5: PFW System: Longitudinal Phase Space keeping the same scale as in Fig. 2.

quadrupole perturbations with the SC force. In the following we will discuss a SC driving term analysis.

## DRIVING-TERM ANALYSIS

An analysis of the Resonance Driving Terms (RDT) coming from the SC potential, using PySCRDT [15], is conducted to try and explain the mechanism that leads to the excitation of the integer resonance in the machine and in MADX-SC [13] simulations. The optics needed for the calculations are taken from the MAD-X twiss files of the PS lattice in two different configurations: a) When the tunes are matched using PFWs, i.e. windings on all of the main magnets that perfectly preserve the periodicity of the machine, and b) when the LEQs, i.e. dedicated quadrupole magnets that are not preserving the periodicity of 50, are used together with the PFWs to control the tune. In normal machine operation, the tune is always controlled using both LEQs and PFWs [16]. The beam characteristics for the calculation of the RDTs are given in Table 1.

Figure 6 shows the evolution of the RDTs due to the SC potential as the integer resonance is approached either using the PFWs (top) or both PFWs and LEQs (bottom). The RDT amplitudes are calculated using:

$$G_{2,0} = -\frac{K_{sc}}{2\pi} \int_0^C \frac{\beta_x}{\sigma_x \cdot (\sigma_x + \sigma_y)} \cdot e^{j(2\phi_x)} ds \quad (1)$$

where,  $K_{sc} = \frac{r_0 N_b}{\beta^2 \gamma^3 \sqrt{2\pi} \sigma_s}$ ,  $r_0$  is the classical particle radius,  $N_b$  the bunch intensity,  $\beta$ ,  $\gamma$  the relativistic factors,  $\sigma_{s,x,y}$  the longitudinal and transverse beam sizes accordingly and  $\phi_x$  the horizontal phase advance. In the PFW case, the periodicity of the machine is not perturbed and as a result the resonance is suppressed by the lattice symmetry. On the other hand, when the LEQs are also used the RDT starts increasing in the proximity of the integer tune at  $Q_x = 6$ . However, once the tune reaches values below  $Q_x < 6.01$ , the RDT seems to drop. To understand this behavior the harmonic analysis of the beam size is needed.

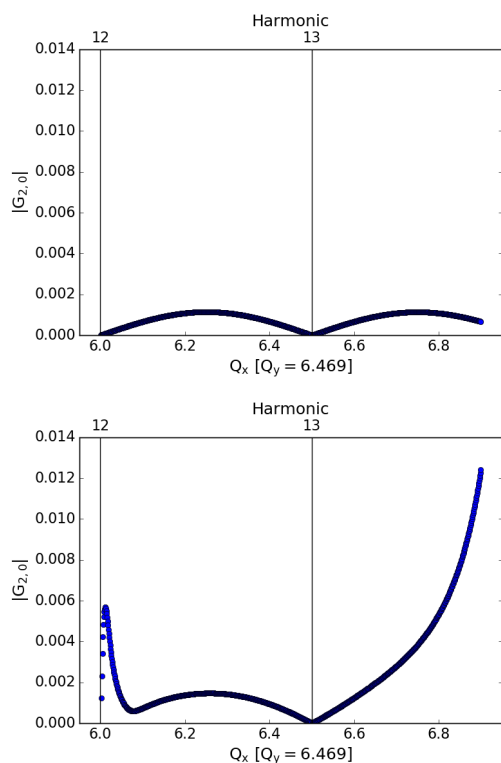


Figure 6: RDT evolution along the horizontal tune  $Q_x$ , when the matching is done using the PFWs (top) and a combination of both PFWs and LEQs (bottom).

The lattice is matched at the nominal working point,  $Q_x = 6.2/Q_y = 6.24$  using the PFWs or the LEQs. The harmonic analysis is presented in Fig. 7 for the different configurations. Using the LEQs, new harmonics are introduced that are suppressed in the fully symmetric lattice. One of the enhanced harmonics is the 12<sup>th</sup> which coincides with the quadrupole resonance at the integer tune  $Q_x = 6$ , i.e. the  $2Q_x = 12$  resonance. These lower order harmonics make it impossible to match the PSB lattice closer to the integer using the LEQs alone.

For the more realistic case of using both PFWs and LEQs, as in the analysis of Fig. 6 (bottom), the harmonic analysis is done at the nominal working point, and closer to the integer resonance as shown in Fig. 8. The combination of both LEQs and PFWs is introducing lower order harmonics but not as many as in the case of LEQs alone. These lower order harmonics, and in particular the harmonic 12, are enhanced substantially as the tune approaches the integer of  $Q_x = 6$ . The harmonic 12 becomes the most important as its amplitude is even larger than the 50<sup>th</sup> harmonic.

In order to understand why the RDT seems to drop when we approach the resonance for  $Q_x < 6.01$  the beam size evolution around the machine is shown in Fig. 9. The beam size is always calculated using the parameters of Table 1. Comparing the beam size for tunes  $Q_x = 6.01$  and  $Q_x = 6.003$  we can see that it has blown up significantly. This means that the SC force, which depends on the beam size,

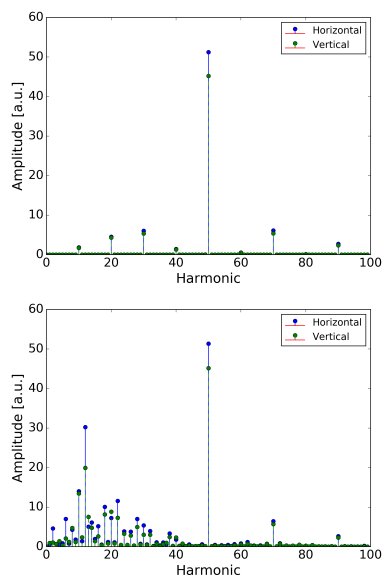


Figure 7: Harmonic analysis of the beam size evolution when the matching is done at  $Q_x = 6.2/Q_y = 6.24$  using the PFWs (top) and LEQs (bottom).

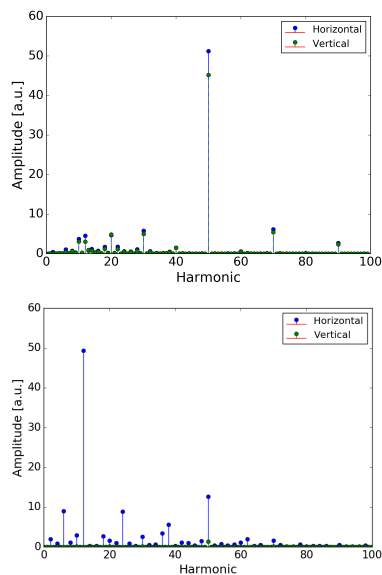


Figure 8: Harmonic analysis of the beam size evolution when the matching is done using both PFWs and LEQs at  $Q_x = 6.2/Q_y = 6.24$  (top) and at  $Q_x = 6.003/Q_y = 6.469$  (bottom).

is significantly reduced. It should be noted that the tune cannot be lowered further when the LEQs and the PFWs are used. Furthermore, the disruption of the optics and the dominance of the 12<sup>th</sup> harmonic can be clearly identified. For completeness the beam size evolution for  $Q_x = 6.001$  when the matching is done using only the PFWs is given. No blow up is observed in this case and the periodicity of 50 is clearly maintained.

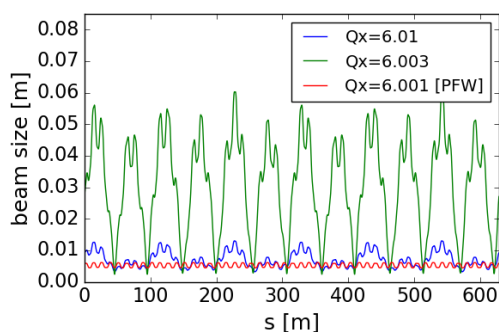


Figure 9: Beam size evolution along the location in the machine while approaching the integer tune. The matching is done using both PFWs and LEQs the  $Q_x = 6.01$  and  $Q_x = 6.003$  cases while for the  $Q_x = 6.001$  only the PFWs are used.

## CONCLUSION

The integer resonance has been studied in the CERN PS in simulations and analytical calculations, in order to better understand the brightness limitation it might impose. The studies revealed that even in the absence of dipole-like errors, which would excite the resonance in 1<sup>st</sup> order, or other random errors in the machine, the resonance can be excited through the disruption of the optics as the integer tune is approached. This disturbance of the machine periodicity leads to 2<sup>nd</sup> order resonance excitation at the integer tune due to space charge.

Further studies may complement what has been described in this report. It would be interesting to analyze the 2<sup>nd</sup> order SC resonance with simulations using PIC codes as no self-consistent analysis has been performed until now. Equally important would be an experimental attempt to approach the PS integer tune without using the LEQs. Moreover, further analysis of the quadrupole RDTs could improve the understanding of the nature of the excitation and quantify the SC contribution.

## ACKNOWLEDGMENTS

The authors would like to thank H. Bartosik for the fruitful discussions.

## REFERENCES

- [1] H. Damerau *et al.*, “LHC Injectors Upgrade, Technical Design Report”, CERN, Geneva, Switzerland, Rep. CERN-ACC-2014-0337, 2014, doi:10.17181/CERN.7NHR.6HGC
- [2] A. Huschauer, “Working point and resonance studies at the CERN Proton Synchrotron,” CERN, Geneva, Switzerland, Rep. CERN-THESIS-2012-212, <http://cds.cern.ch/record/1501943/>.
- [3] G. Franchetti, S. Gilardoni, A. Huschauer, F. Schmidt, and R. Wasef, “Space charge effects on the third order coupled

resonance,” *Phys. Rev. Accel. Beams*, vol. 20, p. 081006, 2017, doi/10.1103/PhysRevAccelBeams.20.081006

- [4] F. Asvesta *et al.*, “Space charge studies in the PS,” *Injector MD Days 2017*, pp. 37–42, 2017, doi:10.23727/CERN-Proceedings-2017-002.37
- [5] R. Wasef, “8th Order Super-Structure Resonance driven by Space Charge,” CERN, Geneva, Switzerland, Rep. CERN-THESIS-2017-455, 2017, <http://cds.cern.ch/record/2670261/>.
- [6] F. Asvesta *et al.*, “Identification and characterization of high order incoherent space charge driven structure resonances in the CERN Proton Synchrotron,” *Phys. Rev. Accel. Beams*, vol. 23, p. 091001, 2020, doi:10.1103/PhysRevAccelBeams.23.091001
- [7] H. Rafique, F. Asvesta, H. Bartosik, A. Huschauer, and M. Kaitatzi, “Approaching the Integer Tune in the Proton Synchrotron to Probe Space Charge at Injection,” Presentation in LIU-PS Beam Dynamics WG meeting #36, 2019, <https://indico.cern.ch/event/857161/>.
- [8] T. Persson, L. Deniau, and G. Roy, “The mad-x program (methodical accelerator design), version 5.07.00,” May 2021, <http://cern.ch/madx/releases/5.07.00/madxguide.pdf>
- [9] A. Latina, S. F. H. Renshall, and Y. Alexahin, “3D symplectic space charge implementation in the latest MAD-X version,” presented at HB’21, Batavia, IL, USA, Oct. 2021, paper MOP21, this conference.
- [10] I. Hofmann and O. Boine-Frankenheim, “Grid dependent noise and entropy growth in anisotropic 3d particle-in-cell simulation of high intensity beams,” *Phys. Rev. ST Accel. Beams*, vol. 17, p. 124201, Dec. 2014, doi:10.1103/PhysRevSTAB.17.124201
- [11] F. Schmidt, “Micro-instability in Space Charge PIC Codes,” Geneva, Switzerland, Apr. 2013, <https://indico.cern.ch/event/221441/>.
- [12] E. Stern, “Synergia Space Charge Benchmarking and Compensation with Electron Lens,” 2nd CERN Space Charge Collaboration Meeting 2018, <https://indico.cern.ch/event/688897/>.
- [13] F. Schmidt and Y. Alexahin, “New SC Algorithm for MAD-X,” CERN, Geneva, Switzerland, Rep. CERN-ACC-2018-0036, 2019, <https://cds.cern.ch/record/2644660/>.
- [14] M. Titze, “Space Charge Modeling at the Integer Resonance for the CERN PS and SPS,” Apr. 2019, <https://edoc.hu-berlin.de/handle/18452/22207/>.
- [15] F. Asvesta and H. Bartosik, “Resonance Driving Terms From Space Charge Potential,” CERN, Geneva, Switzerland, Rep. CERN-ACC-NOTE-2019-0046, 2019, <http://cds.cern.ch/record/2696190/>.
- [16] P. Freyermuth *et al.*, “CERN Proton Synchrotron working point Matrix for extended pole face winding powering scheme,” CERN, Geneva, Switzerland, Rep. CERN-ATS-2010-180, <http://cds.cern.ch/record/1287599/>.